Estimating Sensible Heat Flux from the Oklahoma Mesonet

JERALD A. BROTZGE AND KENNETH C. CRAWFORD

Oklahoma Climatological Survey, University of Oklahoma, Norman, Oklahoma

(Manuscript received 3 August 1998, in final form 12 March 1999)

ABSTRACT

The challenges of using the Oklahoma Mesonet for calculations of sensible heat flux are discussed. The mesonet is an integrated network of 115 remote and automated meteorological stations across Oklahoma that provides the spatial density to observe synoptic and mesoscale features. Temperature and wind speed are measured at two levels at 48 mesonet sites, from which heat flux may be estimated using a gradient approach. A series of field experiments was conducted that quantified the problems and limitations of estimating heat fluxes from the mesonet sites. Four specific problems were identified, and solutions to these limitations are discussed. These problems include 1) differences in instrumentation, 2) an apparent ''offset'' between thermistors, 3) radiative heating error, and 4) fetch limitations. As an independent verification, mesonet flux values were compared directly with eddy correlation estimates.

1. Introduction

Atmosphere–land interaction is a nonlinear process involving heat, mass, and momentum exchange. Spatial variations of surface heat and moisture flux affect cloud formation, precipitation (Clark and Arritt 1995), and temperature distribution (Schwartz and Karl 1990), as well as the formation of nonclassical mesoscale circulations (Segal and Arritt 1992) and thunderstorm initiation (Rabin et al. 1990). Because of limited field observations, however, atmosphere–land interaction, particularly over a heterogeneous surface, is still not well understood.

One reason for this limited understanding is the lack of sufficient observations. Until recently, field programs were relatively few in number because of the stringent accuracy and precision requirements. A great redundancy in the instrumentation was usually needed to maintain accurate results. Experiments were often conducted at a single site such as on an instrumented mast, or on a series of towers spread across a distinctly homogeneous surface. This approach further ensured a consistency of results and allowed for improved quality assurance of the instrumentation. Such field programs included the 1953 Great Plains Experiment, the 1967 Wangara Experiment, and the 1973 Minnesota Experiment (Sorbjan 1989). These experiments were vital in establishing the basic theory and physical dynamics of the planetary boundary layer. Spatial variations and nonlinear interactions of surface fluxes were often neglected, however.

A myriad of bulk and gradient methods have been developed in recent years to derive surface layer fluxes from more conventional atmospheric data. Examples include Priestly and Taylor (1972), Berkowicz and Prahm (1982), Holtslag and Van Ulden (1983), Galinski and Thomson (1995), and Xu and Qiu (1997). The application of these indirect methods, while not as exact as direct methods, allow for routine, cost-effective estimates of surface layer fluxes across a more heterogeneous domain.

Sensible heat flux across Oklahoma can be estimated using a gradient approach with observations of air temperature and wind speed from the Oklahoma Mesonet. The mesonet is an integrated network of 115 remote and automated meteorological stations across Oklahoma that provides the spatial density to observe synoptic and mesoscale features (Brock et al. 1995b). Observations of air temperature and relative humidity (RH) at 1.5 m, wind speed and direction at 10 m, solar radiation, pressure, soil temperature, and precipitation are recorded at all sites every 5 min, whereas soil moisture is recorded every 30 min. In addition, 48 of the 115 sites also measure air temperature (wind speed) at a second level, 9.0 m (2.0 m), providing air temperature and wind speed measurements from two heights. It is at these 48 sites where sensible heat flux could be estimated using a gradient approach. An ongoing and rigorous program of data quality assurance enhances the integrity and quality of mesonet data (Shafer and Hughes 1996) which, in turn, allows for more reasonably accurate estimates of flux.

Corresponding author address: Jerald A. Brotzge, Oklahoma Climatological Survey, University of Oklahoma, 100 E. Boyd, Suite #1210, Norman, OK 73019.
E-mail: jbrotzge@ou.edu

The original goal of this work was to conduct a series of field experiments to demonstrate the feasibility of estimating sensible heat flux using the Oklahoma Mesonet. However, a critical evaluation of the flux estimates revealed several instrumentation/operational problems. By addressing these problems, the entire observational network was improved. The solutions to these problems represent issues that should be considered by all observational networks concerned with improving data quality. These problems are discussed in detail in sections 4–7.

Three separate field experiments were conducted to meet three primary objectives. The first objective was to identify problems and limitations of the mesonet that could limit the accuracy of flux estimates. Second, once problems were identified, solutions to the problems were developed and applied. A third objective was to verify the accuracy of profile flux estimates against estimates produced using an independent system.

2. Theory

A typical mesonet site layout is shown in Fig. 1. Forty-eight sites across Oklahoma are equipped with the apparent capability to estimate heat flux by measuring air temperature and wind speed at two levels (Fig. 2).

Sensible heat flux is estimated using mesonet observations of air temperature at 1.5 and 9 m (z_{t1} and z_{t2}, respectively) and wind speed at 2.0 and 10 m (z_{u1} and z_{u2}, respectively). For purposes of this study and an affiliated effort known as the Oklahoma Atmospheric Surface-layer Instrumentation System (OASIS) Project (Brotzge et al. 1999), a gradient profile method was chosen. This method is based upon Paulson (1970) and modified by T. Horst (1998, personal communication).

The sensible heat flux H (W m^{-2}) can be derived for stable and unstable stratification as

$$H = -\rho C_p(u_* \theta_*), \tag{1}$$

where u_* (m s^{-1}) is the friction velocity, θ_* is a scaling temperature (K), C_p (J K^{-1} kg^{-1}) is the specific heat at constant pressure, and ρ is air density (kg m^{-3}). Next we solve for u_* and θ_*. We begin with the integrated form of the nondimensional gradients of momentum and temperature as described by Paulson,

$$u = \frac{u_*}{k}\left[\ln\left(\frac{z}{z_0}\right) - \psi\left(\frac{z_u}{L}\right)\right] \quad \text{and} \tag{2}$$

$$\theta = \frac{\theta_*}{k}\left[\ln\left(\frac{z}{z_0}\right) - \psi\left(\frac{z_t}{L}\right)\right], \tag{3}$$

where z_0 (m) is the roughness coefficient, ψ_u and ψ_t are the stability functions for momentum and heat, respectively, and L (m) is the Obukhov length. The von Kármán constant (k) has been set to 0.40. Equations (2) and (3) are each applied at the two levels of measurement, z_1 and z_2 (m). The finite difference between levels is then

$$u_2 - u_1 = \Delta\overline{U} = \frac{u_*}{k}\left[\ln\left(\frac{z_{u2}}{z_{u1}}\right) - \psi\left(\frac{z_{u2}}{L}\right) + \psi\left(\frac{z_{u1}}{L}\right)\right] \tag{4}$$

and

$$\theta_2 - \theta_1 = \Delta\overline{\theta} = \frac{u_*}{k}\left[\ln\left(\frac{z_{t2}}{z_{t1}}\right) - \psi\left(\frac{z_{t2}}{L}\right) + \psi\left(\frac{z_{t1}}{L}\right)\right]. \tag{5}$$

The values for u_* and θ_* may then be rewritten as

$$u_* = \frac{k\Delta\overline{U}}{\ln\left(\frac{z_{u2}}{z_{u1}}\right) - \psi_{u2} + \psi_{u1}} \quad \text{and} \tag{6}$$

$$\theta_* = \frac{k\Delta\overline{\theta}}{\ln\left(\frac{z_{t2}}{z_{t1}}\right) - \psi_{t2} + \psi_{t1}}. \tag{7}$$

By substitution of (6) and (7) into (1),

$$H = -\rho C_p\left[k^2\Delta\overline{U}\Delta\left(\frac{\overline{\theta}}{\chi}\right)\right]. \tag{8}$$

The denominator χ is defined as a function of stability. For unstable conditions,

$$\chi = \left[\ln\left(\frac{z_{u2}}{z_{u1}}\right) - \psi_{u2} + \psi_{u1}\right]\left[\ln\left(\frac{z_{t2}}{z_{t1}}\right) - \psi_{t2} + \psi_{t1}\right] \tag{9}$$

and for stable conditions,

$$\chi = \left\{\ln\left(\frac{z_{u2}}{z_{u1}}\right) + \beta\left[\frac{(z_{u2} - z_{u1})}{L}\right]\right\}\left\{\ln\left(\frac{z_{t2}}{z_{t1}}\right) + \beta\frac{(z_{t2} - z_{t1})}{L}\right\}, \tag{10}$$

where β is set equal to 5. The stability functions for momentum (ψ_u) and heat (ψ_t) are defined by Paulson (1970) as

$$\psi_{u(1,2)} = 2\ln\left[\frac{1 + x_{u(1,2)}}{2}\right] + \ln\left[\frac{1 + x_{u(1,2)}^2}{2}\right] + 2\tan^{-1}\left[\frac{1 - x_{u(1,2)}}{1 + x_{u(1,2)}}\right] \quad \text{and} \tag{11}$$

$$\psi_{t(1,2)} = 2\ln\left[\frac{1 + x_{t(1,2)}^2}{2}\right], \tag{12}$$

with

$$x_{u(1,2)} = \left[1 - \gamma\frac{z_{u(1,2)}}{L}\right]^{1/4} \quad \text{and} \tag{13}$$

$$x_{t(1,2)} = \left[1 - \gamma\frac{z_{t(1,2)}}{L}\right]^{1/4}, \tag{14}$$

where $\gamma = 16$, and the Obukhov length is defined as

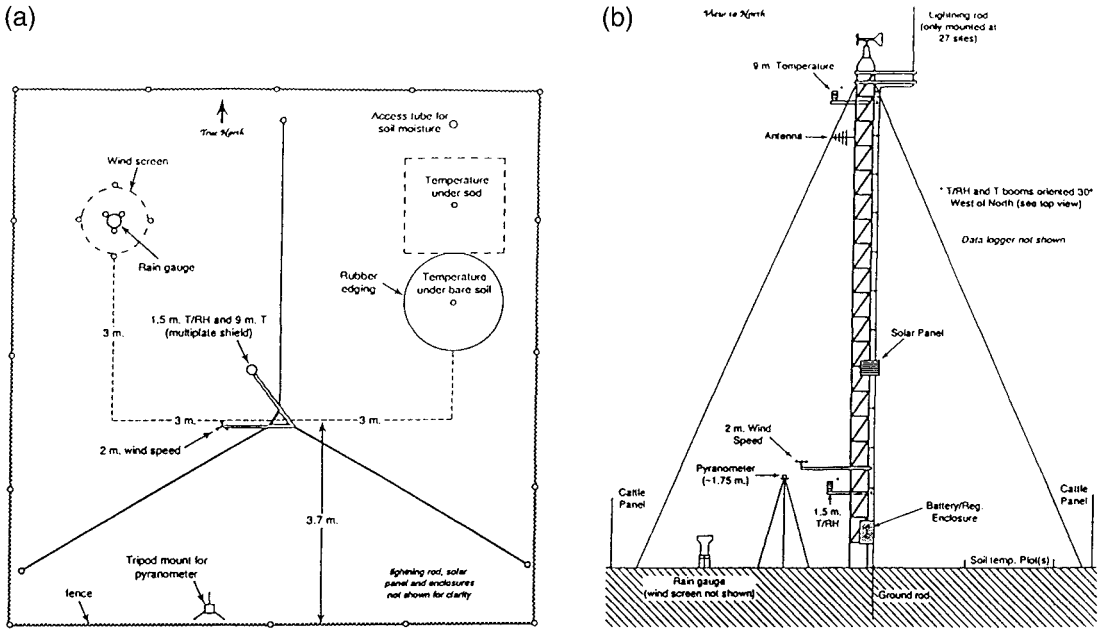

FIG. 1. A typical mesonet site layout: (a) top view and (b) side view from the south. Note that air temperature is measured at 1.5 and 9 m, whereas wind speed is measured at 2 and 10 m.

$$L = \frac{-u_*^3 c_p \rho T_m}{kgH}, \tag{15}$$

where g (m s^{-2}) is the acceleration of gravity, and T_m (K) is the arithmetic mean temperature within the depth of the tower. Equation (13) [Eq. (14)] is applied at each level where wind speeds (temperatures) are measured, in this case at z_{u1} and z_{u2} to yield x_{u1} and x_{u2} (z_{t1} and z_{t2} to yield x_{t1} and x_{t2}).

For unstable conditions, z/L is equivalent to the Richardson number ($z/L \approx \mathrm{Ri}$) when $\phi_h = \phi_m^2$ as explained by Businger (1988):

$$\xi = \frac{z}{L} = \mathrm{Ri}\frac{[\ln(z_{u2}/z_{u1})]^2}{\ln(z_{t2}/z_{t1})}. \tag{16}$$

The Richardson number is calculated in finite difference form as

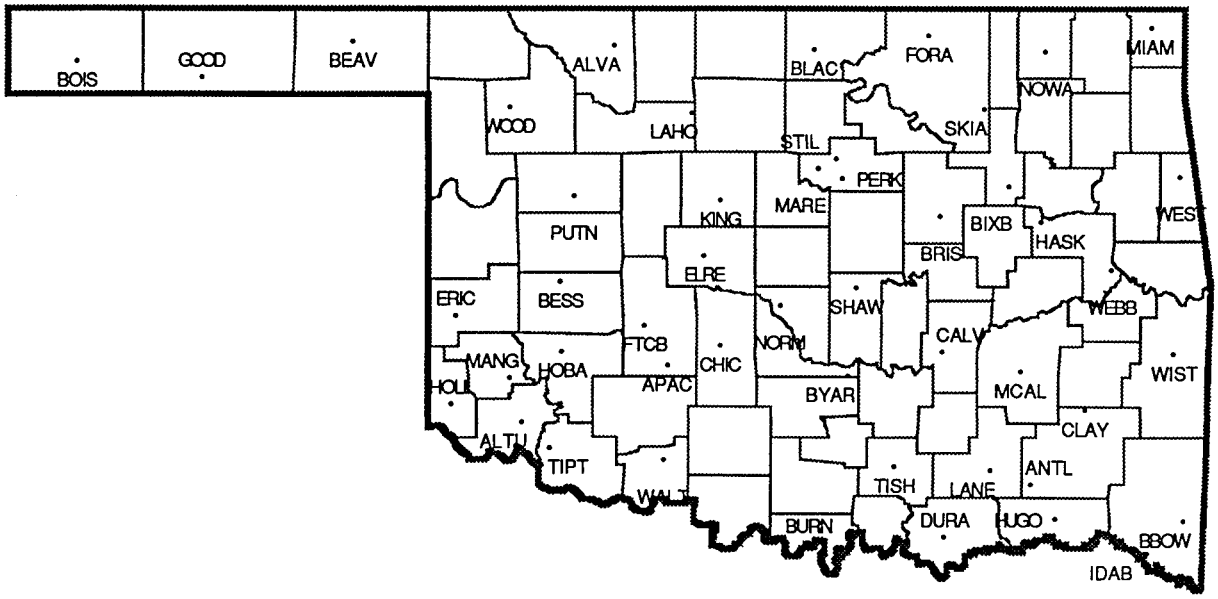

FIG. 2. Oklahoma Mesonet site locations at which temperature and wind speed are measured at two levels, thus enabling sensible heat flux to be estimated.

$$\mathrm{Ri} = \frac{g}{T_m} z_m \frac{\Delta\overline{\theta}}{(\Delta\overline{U})^2}, \tag{17}$$

where z_m (m) is the geometric mean of the temperature measurement height, and $\Delta\overline{\theta}$ (K) and $\Delta\overline{U}$ (m s^{-1}) are the vertical temperature and wind speed gradients, respectively. The geometric mean of the measurement height z_m is defined as

$$z_m = \frac{(z_{u1} z_{u2})}{(z_{t1} z_{t2})^{1/2}}. \tag{18}$$

For stable conditions, ξ is generally not equal to Ri. Because the temperature and wind speed are not measured at the same heights ($z_{u1} \neq z_{t1}$), a quadratic form has been applied:

$$\xi = \frac{-b + \sqrt{b^2 - 4ac}}{2a}. \tag{19}$$

Derived from Eqs. (2) and (3), it can be shown that

$$a = \frac{\beta(z_{t2} - z_{t1})}{z_m} - \mathrm{Ri}\left[\frac{\beta(z_{u2} - z_{u1})}{z_m}\right]^2, \tag{20}$$

$$b = \ln\left(\frac{z_{t2}}{z_{t1}}\right) - 2\mathrm{Ri}\,\ln\left(\frac{z_{u2}}{z_{u1}}\right)\beta\left[\frac{(z_{u2} - z_{u1})}{z_m}\right], \quad \text{and} \tag{21}$$

$$c = -\mathrm{Ri}\left[\ln\left(\frac{z_{u2}}{z_{u1}}\right)\right]^2. \tag{22}$$

If, however,

$$\frac{1}{\beta} > \mathrm{Ri}\left[\frac{(z_{u2} - z_{u1})^2}{z_m(z_{t2} - z_{t1})}\right], \tag{23}$$

then there is no solution, and the flux is undefined.

The gradient method is relatively robust and inexpensive to apply operationally. In addition, the method does not require an explicit estimate of the roughness value (z_0). Because wind speed is only measured at two levels, z_0 cannot be directly estimated. Attempting to calculate z_0 at each site would have relied largely upon empirical relations. Nevertheless, a gradient approach remains highly sensitive to instrumentation error. Heat flux errors at midday could be as large as 100% given a 1°C error in the vertical temperature difference between 1.5 and 9 m.

3. Experimental design

The Oklahoma Mesonet was originally designed in 1991 to provide data that unfortunately are insufficient to permit heat flux calculations through the depth of a 10-m tower. However, to pursue estimates of sensible heat flux across Oklahoma, the operational performance of mesonet sensors needed to be documented so that improved operations could be implemented. Three separate field experiments were conducted from the autumn of 1995 through the summer of 1998.

All three field experiments were conducted at the north base facility of the University of Oklahoma. The north base facility consists of two mesonet towers: the operational mesonet site located in Norman (NORM) and the mesonet's experimental (NEXP) site, located approximately 110 m south of NORM. The NORM tower is fully instrumented as part of the Oklahoma Mesonet; NORM resembles a typical mesonet site as shown in Fig. 1. NEXP is only instrumented on an experimental basis. NORM data are disseminated to the general public as part of the routine mesonet dataset, whereas NEXP data are not publicly disseminated; rather, NEXP is strictly used for the testing and calibration of new instrumentation. NEXP and NORM are centered within a flat, 0.5 km^2 field with unobstructed fetch to the south and east; an interstate highway lies 100 m to the west and small trees lie about 75 m to the north of NORM. Short grasses cover the field, which is kept mowed on a regular basis. The field has a measured albedo of about 15% during midsummer.

Experiment I was conducted between 1 June and 30 September of 1996 at the NORM site. The objective of Experiment I was to install like instrumentation to estimate heat flux more accurately. Currently, air temperature at 1.5 m is measured using a Vaisala HMP35C, whereas the temperature at 9 m is measured using a Thermometrics DC95 (TMM). This first experiment simply included an additional radiation shield and TMM probe at 1.5 m. Thus, the same type thermistor was used at both 1.5 and 9 m and allowed for a more accurate estimate of the vertical temperature gradient. In addition, differences between the HMP35C and TMM, both at 1.5 m, could be monitored. Results from Experiment I are described in sections 4 and 5.

Experiment II had actually been conducted prior to Experiment I between 1 October 1995 and 29 February 1996. The second experiment was repeated during 1 August–31 October 1998. The objective of Experiment II was to quantify the magnitude of the radiation-induced temperature errors in the thermistors used by the mesonet. The mesonet uses nonaspirated radiation shields, which have been documented to produce substantial temperature errors (Richardson 1995). This experiment was designed to quantify these errors. The NEXP tower was instrumented with a series of aspirated and nonaspirated radiation shields, each equipped with a TMM or HMP35C (Fig. 3). An additional aspirated shield (by R. M. Young) and TMM were installed at 1.5 and 9 m as a control. Details from Experiment II are listed in section 6.

Experiment III was conducted between 1 August and 30 September 1998, as part of the OASIS-98 Project (McAloon et al. 1999). Additional instruments were added to NORM to provide a direct comparison between profile and eddy flux measurements (Fig. 4). Cup anemometers were installed at 2 and 9 m; TMM probes were placed at 1.5 and 9 m as in Experiment I. In addition, a CSAT3 sonic anemometer and Krypton hy-

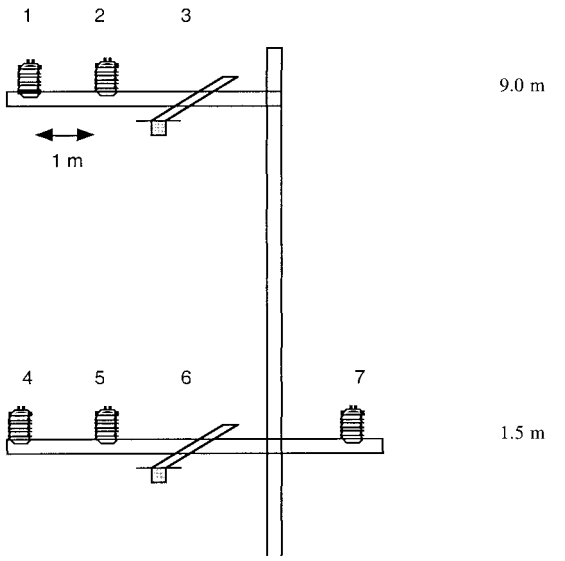

1 Nonaspirated Gill, TMM
2 Aspirated Gill, TMM
3 Aspirated R.M.Young, TMM
4 Nonaspirated Gill, TMM
5 Aspirated Gill, TMM
6 Aspirated R.M.Young, TMM
7 Nonaspirated Gill, HMP35C and TMM

FIG. 3. Experiment II setup, view from the south. The radiational heating error was estimated by comparing aspirated and nonaspirated temperatures.

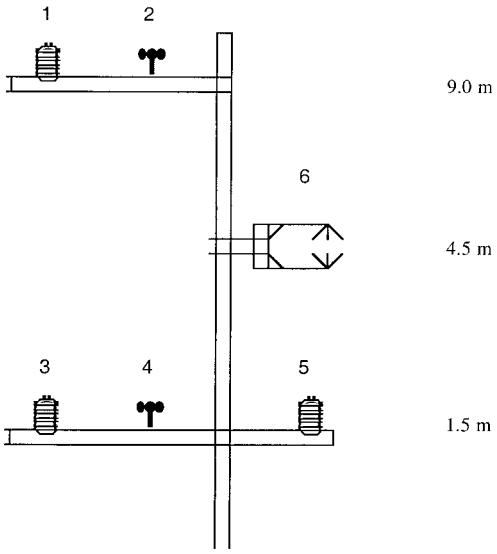

1 Nonaspirated TMM at 9.0 m
2 Cup anemometer at 9.0 m
3 Nonaspirated TMM at 1.5 m
4 Cup anemometer at 2.0 m
5 Nonaspirated HMP-35C at 1.5 m
6 CSI CSAT3 sonic anemometer

FIG. 4. Experiment III setup, view from the south. Profile flux estimates were made from temperature (wind speed) observations at 1.5 and 9 m (2 and 9 m). Eddy correlation estimates were made from the sonic anemometer at 4.5 m.

grometer from Campbell Scientific, Inc. (CSI) were mounted at 4.5 m. Thus, profile and eddy correlation flux estimates could be compared directly. The three field experiments are summarized in Table I.

4. Problem 1: Different instrumentation

Two different types of thermistors were originally chosen by the mesonet to measure air temperature at the 1.5- and 9.0-m levels. A temperature–RH thermistor was used at the 1.5-m level, while a much simpler and cost-effective temperature probe was installed at the 9.0-m level. The 9.0-m probe is a TMM and is small (0.001 m in radius and 0.10 m in length), is silver coated, and has a fast response function. On the other hand, the temperature–RH probe at 1.5 m is an HMP35C, manufactured by CSI and Vaisala. The HMP35C has a much larger thermal mass (0.01 m in radius and 0.25 m in length), is dark colored, and has a slow response time.

In addition, two different types of wind sentries were used to measure wind speed at 2.0 and 10.0 m. A propeller anemometer (model 5103 manufactured by R. M. Young) is used at 10 m and has a starting threshold of about 1 m s^{-1}, and a cup anemometer (model 3101 manufactured by R. M. Young) is used at 2 m and has a starting threshold of about 0.5 m s^{-1}.

The rather significant differences between the two types of thermistors and anemometers used by the mesonet clearly limited the accuracy of flux estimates. As a result, an additional cup anemometer was included at 9.0 m, and a TMM and shield were added at 1.5 m. Thus, the same type of TMM probe placed at 1.5 and 9 m is used to estimate the vertical temperature gradient, and the same type of cup anemometer at 2 and 9 m is used to estimate the vertical wind gradient.

5. Problem 2: "Offset" between thermistors

To quantify the improvement in measuring the vertical gradient of air temperature by using the TMM probes at both levels, a simple field experiment was conducted as described in section 3. Experiment I included a new TMM probe and radiation shield at 1.5 m placed level alongside the HMP35C and shield. The new TMM probe at 1.5 m and its shield were placed on a separate arm that extended east of the tower to minimize wind shadow effects from the tower and other instruments.

A comparison of observations from the TMM and HMP35C at 1.5 m provided a good approximation of the instrument and radiation-induced errors that resulted from a difference in thermistors. However, TMM and HMP35C temperatures, when averaged monthly, produced temperature differences that were much larger than expected and more than that predicted from radiational heating of the sensor (see section 6). A consistent positive (warm) bias was observed by the HMP35C when compared with the TMM (Fig. 5). The cause of the temperature offset did not appear to have been the radiation-induced error documented by Richardson (1995) and Brock et al. (1995a) and indicated by Ex-

TABLE 1. A summary of three field experiments conducted to investigate the feasibility of estimating sensible heat flux from the Oklahoma Mesonet. Instrumentation error was quantified during Experiments I and II. Profile and eddy correlation flux estimates were directly compared during Experiment III.

Experiment	Location	Time period	Instrumentation
I	NORM	1 Jun–30 Sep 1996	Additional shield, TMM at 1.5 m
II	NEXP	1 Oct 1995–29 Feb 1996 1 Aug–31 Oct 1998	Multiple aspirated/nonaspirated shields; TMM/HMP35C temperature probes
III	NORM	1 Aug–30 Sep 1998	Matching shield, TMM at 1.5 and 9 m; cup anemometers at 2.0 and 9 m; sonic anemometer at 4.5 m

periment II. Because all TMM probes had been recently calibrated, the temperature differences uncovered were determined to be a positive offset in the HMP35C observations (see below). A similar comparison of the offset between the HMP35C and TMM at other mesonet sites showed a bias that ranged from 0° to +1.5°C. Fortunately, the temperature offset differences did not vary substantially from month to month.

The newly detected error resulted from conductive interference between the relative humidity and temperature sensors in the HMP35C and the mesonet datalogger. Initially, the datalogger program first recorded the RH followed by the temperature. A laboratory experiment revealed that electrical conductance from the RH observation remained in the probe, which, in turn, interfered with the accuracy of successive temperature measurements (and created the warm offset). Thus, the average HMP35C temperature was in error by greater than 1°C for some sites. The problem had gone undetected in the laboratory and during Experiment II since a separate datalogger program had been used during calibration and testing that only required the temperature measurement from the HMP35C. As a result, the humidity sensor interfered with obtaining accurate temperature observations at field sites—an unfortunate error that previously had not been detected.

The problem was corrected as of 1 March 1997 by reversing the order in which the temperature and RH are measured (Fig. 6). Details of the detected warm bias are described by Fredrickson et al. (1998). Fortunately, the offset of the HMP35C did not directly affect flux estimates with the additional TMM at 1.5 m. However, by adding redundant temperature sensors to the tower, a serious error in the mesonet temperature data was detected and fixed.

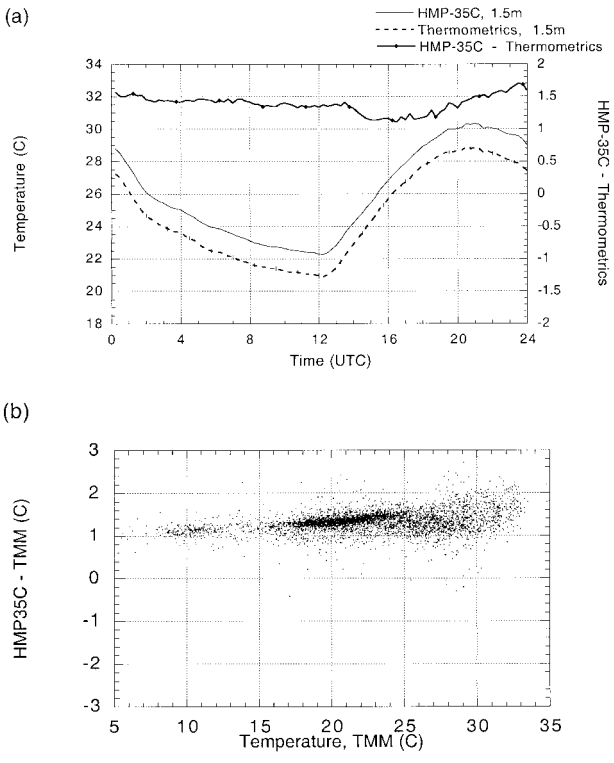

FIG. 5. Temperature measured using the HMP35C and TMM at 1.5 m. (a) Mean difference during Aug 1995 between the HMP35C and TMM as a function of the time of day. (b) Difference between the HMP35C and TMM as a function of air temperature (as measured by the TMM) during Aug and Sep 1995.

6. Problem 3: Radiational heating error

Radiation-induced error is created by the *direct* and *indirect* heating of a sensor placed within a passive solar radiation shield (Richardson 1995). It was determined from laboratory testing and modeling of the observational problem created by the shield design that the radiational heating error was a function of solar radiation intensity and inclination angle, and the wind speed and direction (Brock et al. 1995a). Low solar elevation angle, high surface albedo, and high insolation coupled with low wind speeds represent the primary conditions when shield-induced errors are likely to be significant. The size, thermal conductivity, and absorptivity of each sensor also affect the magnitude of the radiation-induced temperature error. A large, highly absorptive probe likely absorbs more radiation than does a small, highly reflective one. Even with comparable temperature sensors, however, radiational heating errors still limit the ability to obtain accurate flux estimates. Nevertheless, because of limited energy and financial constraints, the mesonet originally chose to use a nonaspirated (i.e., naturally aspirated), Gill-type shield to protect and to ventilate its temperature–RH sensors.

In Experiment II, additional temperature probes and

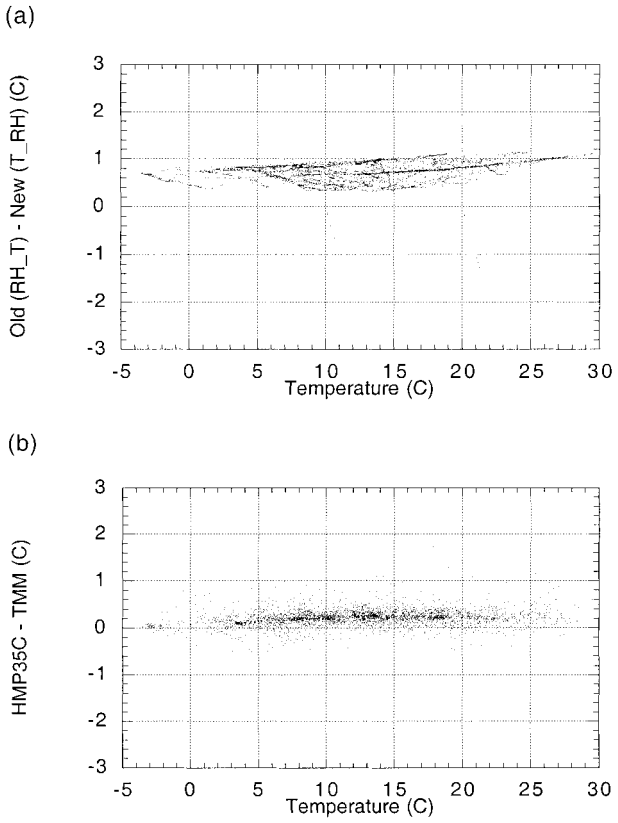

FIG. 6. (a) Temperature difference between the old (relative humidity before temperature, RH_T) and new (temperature before relative humidity, T_RH) methods of measuring the HMP35C air temperature during Mar 1997. (b) Improved temperature between the HMP35C (T_RH) and TMM as a function of air temperature.

radiation shields were placed on the NEXP tower (Fig. 3). A pair of nonaspirated and aspirated shields, each containing a TMM probe, was installed at 1.5 m; a second pair was installed at 9 m. In addition, HMP35C and TMM thermistors were both placed literally in a third nonaspirated shield at 1.5 m. This shield was mounted on a separate arm that extended to the east as shown in Fig. 3 (shield number 7). A small, 12-mV fan powered the aspirated shields, which operated continuously and acted as a control reference. Both the HMP35C and TMM probes were calibrated with respect to an Azonix reference probe.

The objective of Experiment II was to estimate the magnitude of the radiation-induced temperature errors in the thermistors used by the mesonet. First, temperature measurements from the HMP35C and TMM were compared (Fig. 7). Four clear, relatively calm days (3, 7, 10, and 16 October) were chosen as ''worst-case scenarios'' to investigate radiation-induced error. All data represent 5-min averages.

The radiation-induced error was determined to be proportional to the temperature difference between the TMM and HMP35C. The heating error is a function of the size and thermal conductivity of the sensor. Thus, the temperature differences between the probes are equivalent to the induced error resulting only from the differences in the size and thermal characteristics of the sensors.

The radiational heating error was most severe at sunrise; it was evident on all four days. At sunrise, the surface layer was generally stable and wind speeds were at a minimum. The low solar angle combined with minimum wind speeds to produce a consistent and significant (>1°C) error at sunrise. This large temperature difference lasted over 1 h in most cases. Wind speeds generally less than 2 m s^{-1} created conditions whereby radiation-induced errors could become large. As wind speeds increased, the temperature difference approached zero.

Radiational cooling effects may have caused substantial temperature differences between the two sensors at night. With wind speeds less than 1 m s^{-1}, temperature differences as large as 0.5°C were observed.

On a monthly basis, the diurnal averages (Fig. 8) contained radiation-induced errors that appeared to be a function of radiation intensity. For example, the maximum difference in observations from the two sensors decreased to a minimum value in December; it increased in January and February. Even so, the most prominent temperature differences still occurred at sunrise.

Next, temperature measurements were compared from the TMM probes placed inside aspirated and nonaspirated shields. A comparison of the aspirated and nonaspirated TMMs for each of the four clear, calm days is shown in Fig. 9.

The 3 October data clearly show the radiation-induced error at sunrise. On 7 October, a long night of calm winds combined with the sunrise radiation to produce a large error in excess of 2°C. The direct effect of wind speed on the temperature error was most clearly evident in the 10 October data. Wind speeds decreased three separate times, and each time an increase in radiational errors resulted. As wind speeds decreased, temperature errors increased. The 16 October data showed a similar pattern. A nocturnal difference of -0.2°C was the product of heat advected from fans in the aspirated shields. The 9.0-m data showed similar results.

Wind speed differences at 1.5 and 9.0 m create different radiation-induced errors, however. The temperature error is a function of wind speed that varies with measurement height. Larger wind speeds at 9 m reduce radiational errors while lower wind speeds at 1.5 m lead to higher radiational errors. This error adversely creates a significant positive bias in heat flux estimates when using a vertical temperature gradient. Data collected during August 1998 revealed a bias of approximately 16.4% (Fig. 10).

To reduce radiative heating error, a correction algorithm has been developed. A similar model was developed independently by Anderson and Baumgartner (1998) and was applied to naturally ventilated thermistor

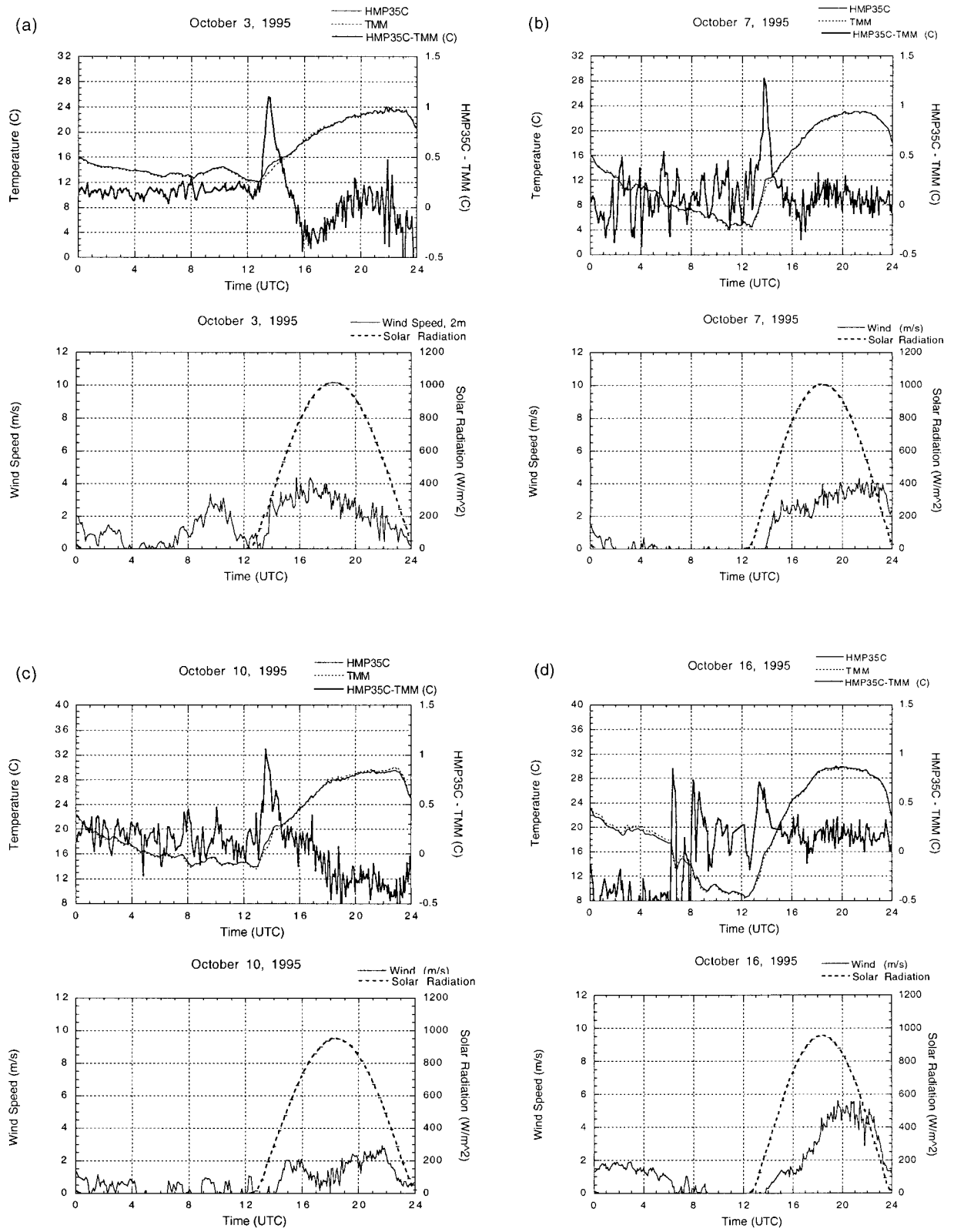

FIG. 7. Radiation-induced temperature differences between nonaspirated sensors (HMP35C − Thermometrics; °C) observed on 3, 7 (top) and 10, 16 (bottom) Oct 1995.

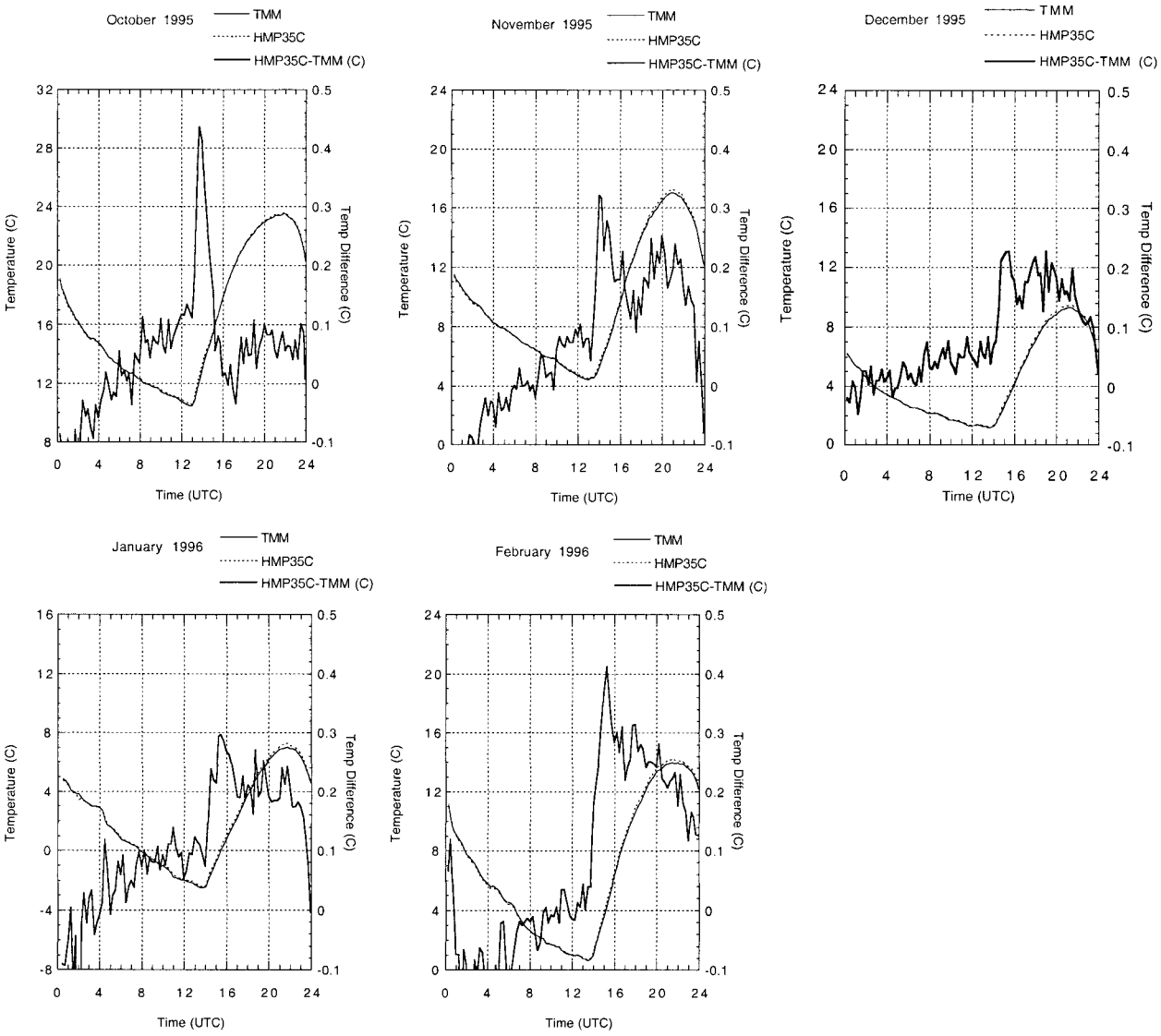

FIG. 8. Radiation-induced temperature differences (HMP35C − Thermometrics; °C) averaged on a monthly basis from Oct 1995 through Feb 1996.

temperatures measured from buoys. The radiation-induced error is directly proportional to the solar radiation and inversely proportional to the wind speed and solar elevation angle. A linear superposition of these physical parameters forms the ratio

$$\alpha = \frac{Q(1.1 - 0.6 \sin\phi)}{(1.0 + U)^2}, \tag{24}$$

where Q is solar radiation (W m^{-2}), ϕ is the solar elevation angle, and U is wind speed (m s^{-1}). The ratio α, which varies proportionally to the radiation-induced error, is empirically adjusted to a simple polynomial fit to yield a final temperature correction

$$\Delta T = a + b\alpha + c\alpha^2 \quad \text{and} \tag{25}$$

$$T_{\text{new}} = T_{\text{obs}} - \Delta T, \tag{26}$$

where $a = 0.0299$ (K), $b = 0.003\,860\,3$ (W^{-1} m^4 s^{-2} K), and $c = 4.6348e^{-6}$ (W^{-2} m^8 s^{-4} K), T_{obs} is the observed air temperature, and T_{new} is the corrected air temperature. The algorithm is applied separately at each vertical level: 1.5 and 9 m. An examination of flux estimates using the correction algorithm showed improved fluxes by approximately 6%.

7. Problem 4: Fetch limitations

Fetch may be a problem at selected sites, particularly in eastern Oklahoma. Nearby trees and tall grasses are known to obstruct a proper fetch at a few sites. Special attention was given to locate and install all stations in a similar manner so that they were consistent with World Meteorological Organization standards. The site of each

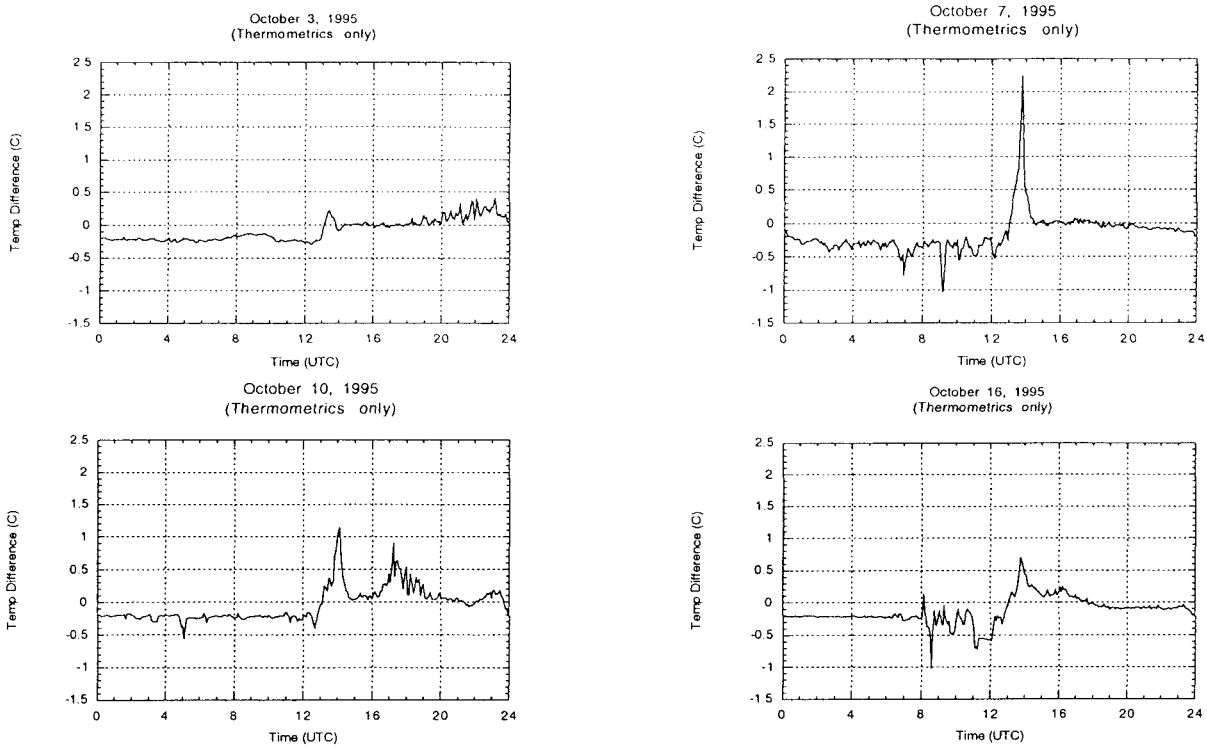

FIG. 9. Radiation-induced temperature differences between nonaspirated and aspirated TMMs (nonaspirated − aspirated; °C) for 3, 7 (top) and 10, 16 (bottom) Oct 1995.

station was as representative as possible of the surrounding region. However, data communication requirements and natural terrain features compromised standards at a few locations. Guidelines for site placement were developed by a site standards committee and are described in detail by Shafer et al. (1993).

A close examination of data from nine selected sites across the mesonet revealed that about one-third of the sites experienced some fetch interference from either trees or tall vegetation. One southeastern Oklahoma site, Broken Bow, which is located in a national forest, appeared to have winds significantly smaller because of nearby trees. Tall vegetative growth at two eastern Oklahoma sites, Webbers Falls and Tishomingo, appeared to have retarded the 2-m winds on some occasions and, as a result, may have significantly affected heat flux estimates.

8. Comparison of profile versus eddy correlation estimates

To validate the methodology used to estimate sensible heat flux, mesonet estimates were compared with fluxes derived from an independent system. A collocated eddy correlation system was established to serve as an independent source to assess the accuracy of flux estimates at mesonet sites. Instruments for use with both the profile and eddy correlation systems were mounted on the same tower to minimize fetch differences. Flux estimates from both systems were compared during August and September of 1998 at the Norman site as described in section 3.

Four clear days were chosen from two months of collected data to highlight the challenges and promise of estimating heat fluxes using data from the mesonet. During 29 and 30 August, light to calm wind conditions prevailed with temperatures near 40°C (Fig. 11). The period represented a worst-case scenario for radiation-induced errors. During 20 and 25 September, however, wind speeds remained >4 m s^{-1} during the day, which reduced radiational heating errors and improved the agreement between profile-eddy correlation (Fig. 12). All data shown are 15-min averages of 5-min observations.

The high solar radiation/low wind speed conditions of 29 and 30 August created the worst agreement between the profile and eddy correlation estimates during the entire two-month study. Many of the 15-min averages differed by more than 200 W m^{-2}. As described in section 6, low wind speeds lead to an overestimate of the air temperature and thus to an overestimate of the heat flux. The data from 30 August best highlight the impact of radiation-induced errors. As wind speeds increase during the day, the profile and eddy systems gradually converge as the profile estimates presumably improve. The mean difference between the two methods was 44 W m^{-2} with a standard deviation of 63 W m^{-2}.

A slight increase in wind speeds on 20 and 25 Sep-

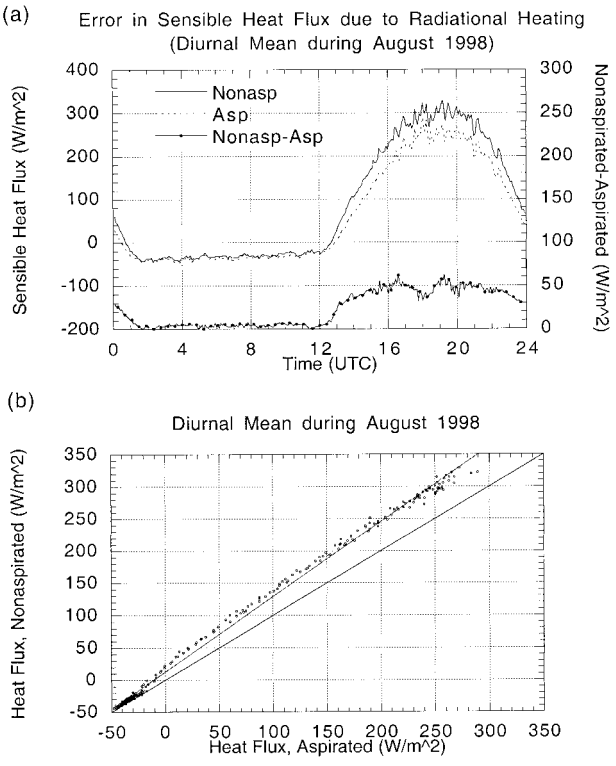

FIG. 10. Sensible heat flux estimated using nonaspirated TMM probes compared with heat flux estimated using aspirated TMM probes. (a) Monthly diurnal cycle of heat flux using nonaspirated and aspirated TMM probes. (b) Sensible heat flux estimated using nonaspirated versus aspirated TMM probes.

tember lead to improved agreement between the profile and eddy correlation methods. Wind speeds of 4–5 m s^{-1} on 20 September reduced the errors due to radiational heating, yielding an average difference of 21 W m^{-2} between the two flux methods. However, a wind speed of about 6 m s^{-1} on 25 September reduced the mean difference between the two methods to 6 W m^{-2} with a standard deviation of 13 W m^{-2}. A scatterplot of all data observed during the four clear days is shown in Fig. 13a. The profile estimates are approximately 10% higher than those observed from eddy correlation. Many of the outliers are removed when data are excluded when winds were less than 2 m s^{-1} (Fig. 13b); however, profile estimates remained about 10% higher than eddy correlation estimates.

All 5-min observations collected during the entire month of August are shown in Fig. 14. Profile estimates during August are observed to be about 17.6% higher than eddy correlation estimates; the differences were reduced to 11% by applying a correction for radiative heating errors. Interestingly, the observed mean difference between the aspirated and nonaspirated profile estimates during August was 16.4% (Fig. 10). A similar examination of data collected between 13 and 28 September, however, revealed a much smaller difference of approximately 6.5%; the correction for radiative heating errors reduced differences to 0.35%. The mean difference between the profile and eddy correlation estimates was only 6 W m^{-2}. In general, because September was windier and cloudier than August, radiational heating errors were much smaller, which, in turn, improved profile flux estimates. The clear skies and light winds experienced during August are considered to represent the worst-case conditions to be expected.

9. Conclusions

The objective of this study was to assess the problems and challenges of using Oklahoma Mesonet data for estimating heat fluxes. As a result, the problems of estimating heat flux have been identified, reasonable solutions have been formulated, and in some cases the problems have been eliminated. In the process, the quality of mesonet data has been improved because flux estimates are based upon more precise and accurate measurements.

The Oklahoma Mesonet represents a unique resource to monitor boundary layer fluxes over a large spatial domain. Before flux estimates from the mesonet can be used for research purposes, however, the problems and challenges of using mesonet data for flux calculations had to be documented and the resulting error levels established. The principal results of our investigation follow.

1) Identical instrumentation must be installed at the two levels on mesonet towers for accurate flux estimates to be made. The HMP35C and TMM sensors often differed by more than 0.25°C due to radiational heating problems. The starting thresholds of the two different anemometers varied, which introduced error at low wind speeds (and thus at low flux values).
2) A systematic temperature error created by the mesonet's datalogger was corrected as of 1 March 1997. The temperature bias resulted from conductive interference between the 1.5 m HMP35C and the datalogger and ranged from near zero to nearly 1.5°C.
3) Radiational heating errors were found to be a function of the magnitude of solar radiation and the solar elevation angle as well as wind speed and direction. Temperature errors from the TMM ranged from near zero to +2.0°C; temperature errors from the HMP35C ranged from near zero to about +2.5°C. Because the mesonet uses a passive shield, the errors were limited to clear, calm periods, such as often occur at sunrise. The impact of radiation-induced errors is an overestimate of heat flux—often by as much as 15%.
4) Fetch interference affects flux estimates at a few mesonet sites. Tall grasses and dense vegetation, particularly in eastern Oklahoma, have been shown to reduce wind speeds at 2 m and thereby reduce the estimates of heat flux.
5) A two-month comparison between profile method

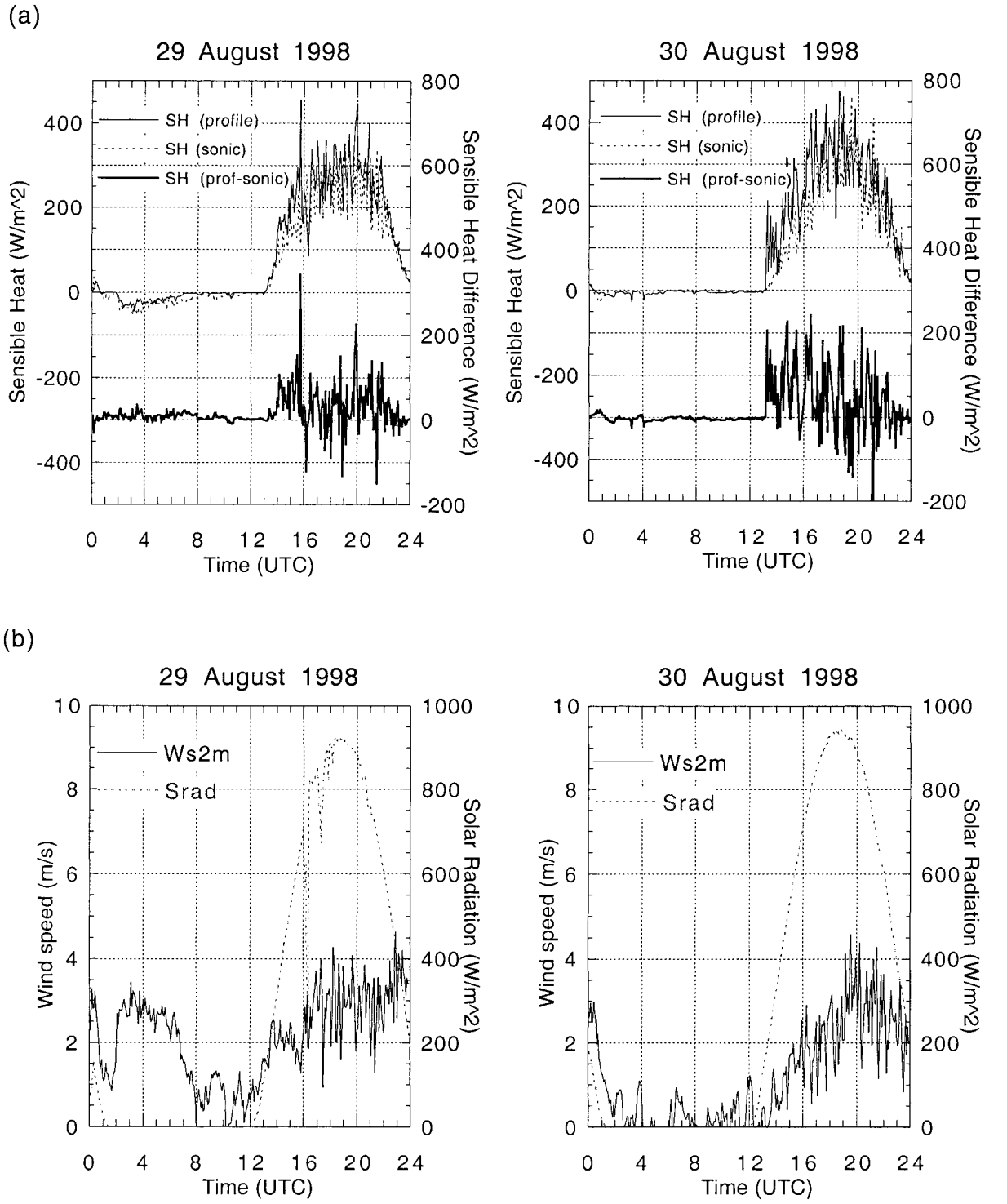

FIG. 11. (a) Sensible heat flux estimated from both profile and eddy correlation methods for 29 and 30 Aug 1998. (b) Solar radiation and wind speed observations for 29 and 30 Aug 1998.

and eddy correlation measurements revealed reasonably good agreement between the two methods under most conditions. Profile estimates tended to overestimate heat flux by about 15% during August and by approximately 6% during September. Most errors appear to be caused by the radiational heating problem. Observations collected during August represented worst-case conditions.

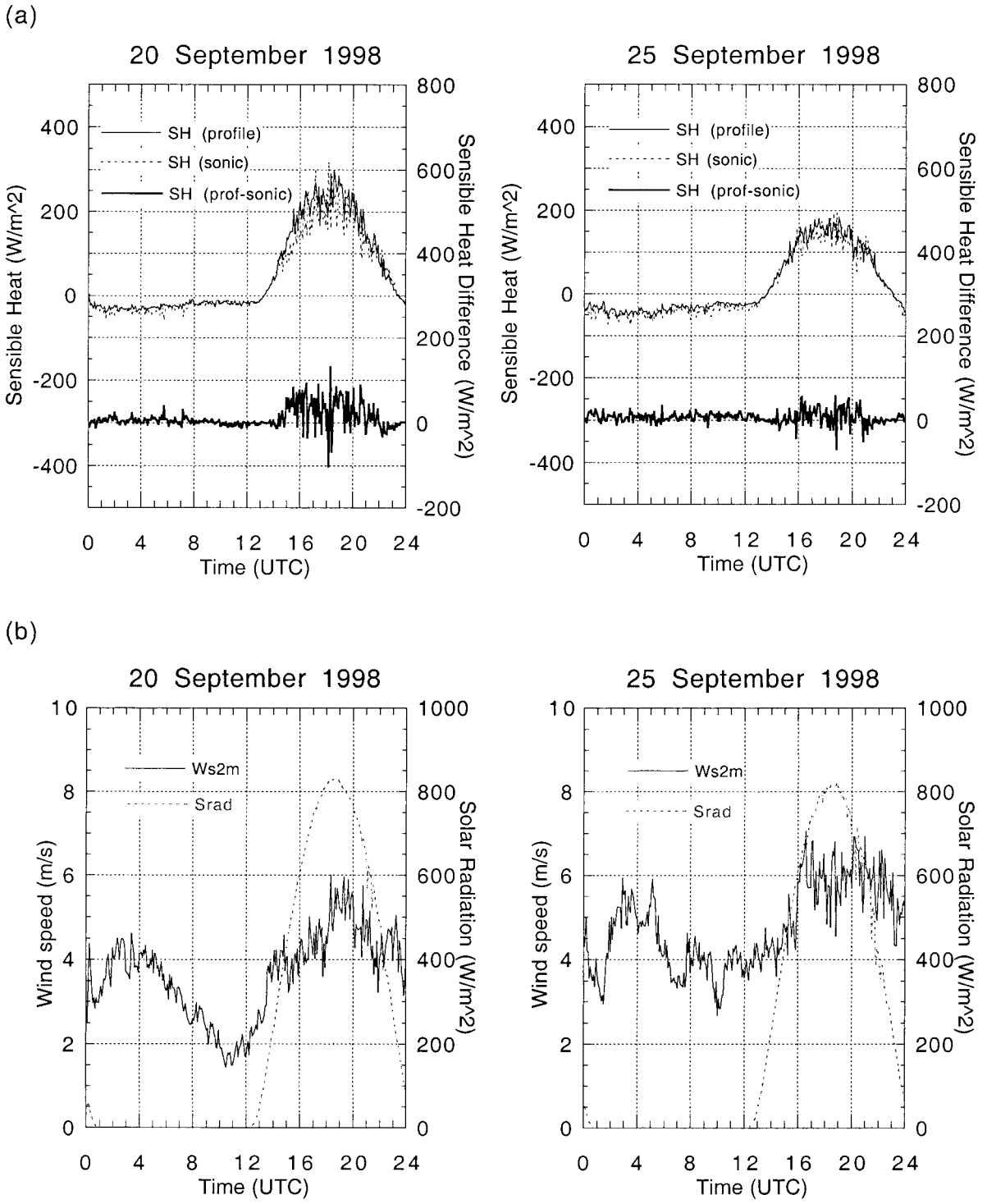

FIG. 12. (a) Sensible heat flux estimated from both profile and eddy correlation methods for 20 and 25 Sep 1998. (b) Solar radiation and wind speed observations for 20 and 25 Sep 1998.

6) A correction algorithm was developed to minimize radiational heating errors. Improved temperature measurements lead to an approximate 6% improvement in profile flux estimates. Additional work is recommended in developing and refining a correction to further minimize radiational heating errors.

Promising results reveal that heat fluxes can be es-

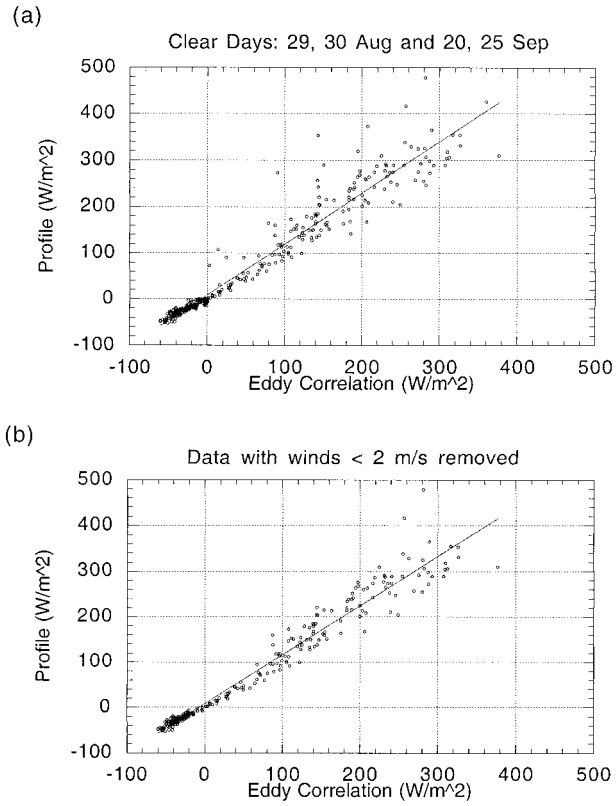

FIG. 13. (a) Eddy correlation versus profile method of estimating sensible heat flux for the four clear days chosen during Experiment III. (b) Same plot as in (a), but data were removed when wind speeds were < 2 m s^{-1}.

timated within reasonable accuracy, provided the instrumentation and operational corrections are applied as described in this study. Since such changes have been made, large-scale flux estimates can be monitored in real time across the entire Oklahoma Mesonet.

Acknowledgments. This research was made possible, in part, by NSF Grant 125-5645. The authors would like to thank Dr. Zbigniew Sorbjan from Marquette University, Department of Physics, for proposing much of this project. Thanks to Sherman Fredrickson and David Grimsley for all their effort, and the field technicians of the Oklahoma Mesonet Project for their professional assistance in maintaining our ongoing, experimental activities. Also, a special thanks to Tom Horst (NCAR) for his expertise and insightful discussions, and to NCAR for the use of the ISFF facility and personnel during OASIS-98.

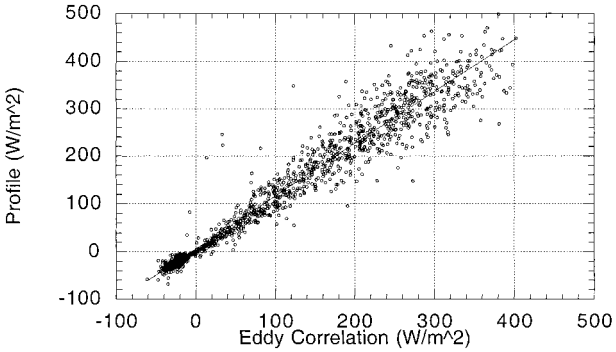

FIG. 14. Eddy correlation versus profile method of estimating sensible heat flux for the month of Aug. Values represent 15-min averages from 5-min observations.

REFERENCES

Anderson, S. P., and M. F. Baumgartner, 1998: Radiative heating errors in naturally ventilated air temperature measurements made from buoys. *J. Atmos. Oceanic Technol.*, **15,** 157–173.

Berkowicz, R., and L. P. Prahm, 1982: Sensible heat flux estimated from routine meteorological data by the resistance method. *J. Appl. Meteor.,* **21,** 1845–1864.

Brock, F. V., S. J. Richardson, and S. R. Semmer, 1995a: Passive multiplate solar radiation shields. Preprints, *Ninth Symp. on Meteorological Observations and Instrumentation,* Charlotte, NC, Amer. Meteor. Soc., 329–334.

——, K. C. Crawford, R. L. Elliott, G. W. Cuperus, S. J. Stadler, H. L. Johnson, and M. D. Eilts, 1995b: The Oklahoma Mesonet: A technical overview. *J. Atmos. Oceanic Technol.,* **12,** 5–19.

Brotzge, J. A., S. J. Richardson, K. C. Crawford, T. W. Horst, F. V. Brock, K. S. Humes, Z. Sorbjan, and R. L. Elliot, 1999: The Oklahoma Atmospheric Surface-Layer Instrumentation System (OASIS) Project. Preprints, *13th Symp. on Boundary Layers and Turbulence,* Dallas, TX, Amer. Meteor. Soc., 612–615.

Businger, J. A., 1988: A note on the Businger–Dyer profiles. *Bound.-Layer Meteor.,* **42,** 145–151.

Clark, C. A., and R. W. Arritt, 1995: Numerical simulations of the effect of soil moisture and vegetation cover on the development of deep convection. *J. Appl. Meteor.,* **34,** 2029–2045.

Fredrickson, S., J. A. Brotzge, and D. Grimsley, 1998: If everything checks out so well how can the data still be bad? Preprints, *10th Symp. on Meteorological Observations and Instrumentation,* Phoenix, AZ, Amer. Meteor. Soc., 343–348.

Galinski, A. E., and D. J. Thomson, 1995: Comparison of three schemes for predicting surface sensible heat flux. *Bound.-Layer Meteor.,* **27,** 345–370.

Holtslag, A. A. M., and P. Van Ulden, 1983: A simple scheme for daytime estimates of the surface fluxes from routine weather data. *J. Climate Appl. Meteor.,* **22,** 517–529.

McAloon, C. M., S. J. Richardson, J. A. Brotzge, and T. W. Horst, 1999: Preliminary results from the OASIS-98 field project. Preprints, *13th Symp. on Boundary Layers and Turbulence,* Dallas, TX, Amer. Meteor. Soc., 616–619.

Paulson, C. A., 1970: The mathematical representation of wind speed and temperature profiles in the unstable atmospheric surface layer. *J. Appl. Meteor.,* **9,** 857–861.

Priestley, C. H. B., and R. J. Taylor, 1972: On the assessment of surface heat flux and evaporation using large-scale parameters. *Mon. Wea. Rev.,* **100,** 81–92.

Rabin, R. M., S. Stadler, P. J. Wetzel, D. J. Stensrud, and M. Gregory, 1990: Observed effects of landscape variability on convective clouds. *Bull. Amer. Meteor. Soc.,* **71,** 272–280.

Richardson, S. J., 1995: Multiple radiations shields: Investigating radiational heating errors. Ph.D. dissertation, University of Oklahoma, 134 pp. [Available from 100 E. Boyd, Suite 1210, Norman, OK 73019.]

Schwartz, M. D., and T. R. Karl, 1990: Spring phenology: Nature's experiment to detect the effect of ''green-up'' on surface maximum temperatures. *Mon. Wea Rev.,* **118,** 883–890.

Segal, M., and R. W. Arritt, 1992: Nonclassical mesoscale circulations

caused by surface sensible heat-flux gradients. *Bull. Amer. Meteor. Soc.,* **73,** 1593–1604.

Shafer, M. A., and T. W. Hughes, 1996: Automated quality assurance of data from the Oklahoma Mesonetwork. Preprints, *12th Int. Conf. on Interactive Information and Processing Systems for Meteorology, Oceanography, and Hydrology,* Atlanta, GA, Amer. Meteor. Soc., 340–343.

——, ——, and J. D. Carlson, 1993: The Oklahoma Mesonet: Site selection and layout. Preprints, *Eighth Symp. on Meteorological Observations and Instrumentation,* Anaheim, CA, Amer. Meteor. Soc., 231–236.

Sorbjan, Z., 1989: *Structure of the Atmospheric Boundary Layer.* Prentice Hall, 317 pp.

Xu, Q., and C.-J. Qiu, 1997: A variational method for computing surface heat fluxes from ARM surface energy and radiation balance systems. *J. Appl. Meteor.,* **36,** 3–11.